Fringe envelope tracking at COAST

Nathalie D. Thureau[a†], Roger C. Boysen[a], David F. Busher[a], Christopher A. Haniff[a], Ettore Pedretti[b‡], Peter J. Warner[a] and John S. Young[a]

[a]Astrophysics Group, Cavendish Laboratory, Madingley Road, CB30HE, Cambridge, UK
[b]Harvard-Smithsonian Center for Astrophysics, 60, Garden Street, MS20, Cambridge, MA 02138, USA

ABSTRACT

We report on a new fringe envelope tracking system installed at the Cambridge Optical Aperture Synthesis telescope (COAST). This currently uses the existing photon-counting avalanche photo diode (APD) detector system to allow real-time fringe tracking on up to 3 baselines simultaneously. This system has been recently tested on the sky and has proved to successfully track the fringe envelope on a 38m baseline. The algorithm based on an envelope method has also been implemented and tested at the Infrared-Optical Telescope Array (IOTA) interferometer.

Keywords: interferometry, fringe envelope tracking

1. INTRODUCTION

COAST[1] is an imaging interferometer which provides fringe visibility measurements that can be used to reconstruct images. It is a Y-shaped array which consists of 5×40cm telescopes. It has two beam combiners, one operating in the visible part of the spectrum ($650 - 1000$nm), the other one operating in the near infrared ($1.3 - 2.2\mu$m) (see Fig. 1). The equalisation of the optical paths is carried out by four delay lines, each consisting of a roof mirror mounted on a motorised trolley running on 30m rails.

In order to obtain interference between any two telescopes, the difference in optical path travelled by the two beams of light must be matched to less than the coherence length of the light being observed, typically a few microns. For ground-based long-baseline optical and infrared interferometers, the Earth's atmosphere introduces random path-length fluctuations of many tens of microns with a timescale as short as a few milliseconds.

The basic idea for a fringe envelope tracking system at COAST was to have a system that can take the output of any of the beam combiner in order to sense and correct atmospherically-induced disturbances to the optical pathlength inside the interferometer.

The results presented in this paper concentrate on the implementation of the fringe envelope tracker for the visible beam combiner. We present the principle of the system, its implementation at COAST and the first tests carried out on the sky.

2. DESCRIPTION OF THE HARDWARE

The light beams coming out from the telescopes are fed into the delay lines where the optical paths are equalised by moving the trolleys. Their positions are controlled by a two stage system. The high frequency errors are corrected by moving the voice-coil-controlled roof mirror with respect to the trolley. The low frequency large displacements are provided by motion of the trolleys. The accuracy of the trolley position is ensured by the use of a laser interferometer system.

The beams are then fed into one of the two beam combiners which can accept up to 4 beams. Each combiner generates four collimated outputs that are focused onto single pixel detectors which record the photon counts versus time. In the visible, the detectors are optical APDs[2] , whereas in the near infrared, they are single pixels

† Marie Curie postdoctoral fellow, ‡Smithsonian Predoctoral Fellow
Further author information: (Send correspondence to N.D.T)
N.D.T.: E-mail: thureau@mrao.cam.ac.uk

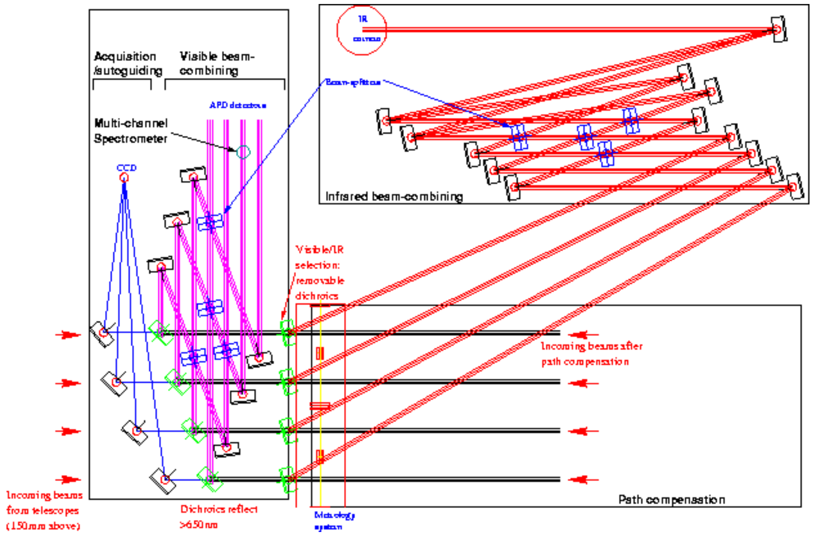

Figure 1. The 4-way all-in-one visible and near infrared beam combiners.

from a NICMOS III detector.[3]
By sweeping the roof mirror position back and forth, we change the optical path length, producing temporally encoded interference fringes. The path length is varied in a symmetric triangle wave of frequency 5Hz, meaning that there are 10 sweeps per second. The temporal modulation in the fringe pattern intensity appears as a sinc function, "the fringe envelope", multiplied by a cosine function, "the fringes". The centre of the fringe envelope indicates the position of the roof mirror which equalises the optical path between the different beams. The length of the sweep is typically 60 microns which is longer than the coherence length of the optical filter bandpasses ($\sim 20-40$nm bandpass corresponds to $\sim 40-80$ fringes at 800nm) used for fringe tracking.
For closure phase measurements, the light from three telescopes is combined simultaneously. The path length is modulated in a similar fashion as before, but at a different speed in each arm. This serves to separate the fringes from each baseline in frequency (see Fig. 2).
In the optical band, we use the APD output signal for fringe tracking. It consists of a stream of digital pulses

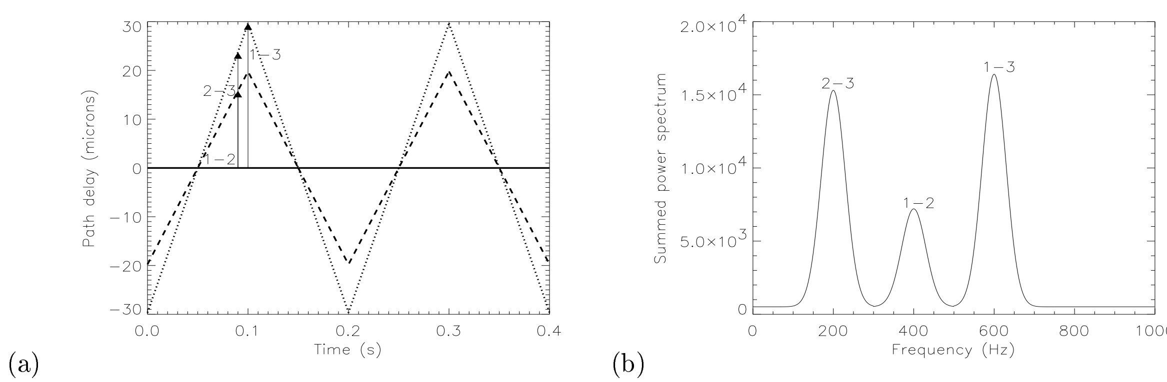

Figure 2. (a) Optical path delay as a function of time for a 3-beam temporally-scanned combination. Each line represents the path delay in one arm. Plain line: trolley 1 with a zero sweep amplitude, dashed line: trolley 2, dotted line: trolley 3. The fringes appear at 1 (beams 2 and 3), 2 (beams 1 and 2) and 3 (beams 1 and 3) times the fundamental fringe frequency. (b) The corresponding power spectrum. The three peaks due to the fringes on three different baselines can clearly be seen. The higher the sweep amplitude, the higher the fringe peak frequency.

corresponding to photon arrival times. The pulses are counted by an ISA card in the PC. A driver running under RT-Linux (real-time Linux) reads the 4 counters at 200-microsecond intervals and saves the readings to a memory buffer. Every sweep (i.e. every 100ms) the data is transferred to a data manager which makes data available to a normal user-space Linux process where the fringe envelope tracking software is installed. At COAST we use different filters in front of the different APDs, which enable us to use broadband filters for fringe tracking and narrowband filters for science observations.

3. OVERVIEW OF THE FRINGE ENVELOPE TRACKING SYSTEM

We give in Fig. 3 a block diagram representation of the fringe envelope tracking software. This diagram summarises the main functions involved in the fringe envelope tracking process.
A set of detectors records the intensity coming out from either the visible or the infrared beam combiners. The fringe tracking software send a data request to the data manager via a socket link. If data are available, the data manager sends back a chunk of data and a header which include all the information relevant for the interpretation of the data by the tracking system.
Then the program extracts the signal from the APD used for fringe tracking. It computes the power spectrum of the interferogram and performs a test on the power spectrum to check the presence of the fringe peak(s) in the power spectrum. If no fringe peak can be detected, the program processes the next data until a fringe peak has been found. However, if a fringe peak is detected, it calculates the fringe envelope and estimates its mean position.
The COAST control software "ApdGui" provides a real-time display with interactive plots of either the raw data, the power spectrum or the fringe envelope. Thus we got a real time visual display of the current fringe packet position.
The envelope position is computed using the algorithm described below and this is converted into trolley offsets which are made available to the trolley controller through a serial port link. The trolley controller reads the serial line and places the values in the common data area and a flag is set. An interrupt routine is called every 0.2ms and every 0.2ms the position of each trolley is updated. Any offsets from the envelope tracking system are added to the trolley positions.
This closed loop system works as an integral controller which output is proportional to the integral of the error with time. The gain of the control can be adjusted, so as to adapt the system to different light level or atmospheric conditions.

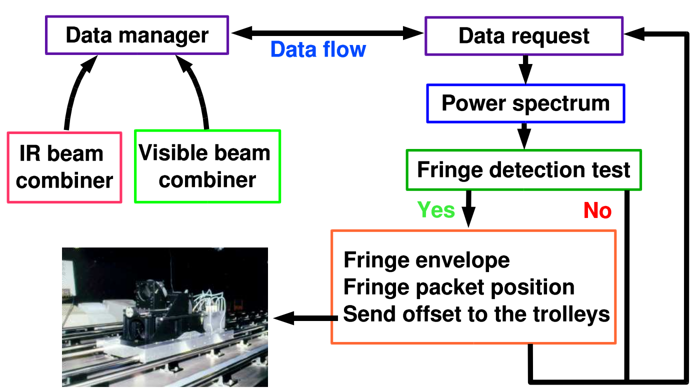

Figure 3. Block diagram of the fringe envelope tracking software

4. DESCRIPTION OF THE SINGLE-CHANNEL ENVELOPE DETECTION ALGORITHM

We give in this section a detailed description of the algorithm used to calculate the fringe envelope and find the null-OPD (Optical Path Delay) point in a fringe packet.

The algorithm takes a fringe template which is a sinusoid modulated by a roughly Gaussian envelope (see Fig. 4.a) and slides this template across the data, determining the correlation coefficient as a function of the template position. The frequency of the sinusoid is the central frequency of the fringes and the width of the Gaussian corresponds to the inverse of the frequency range over which we wish to average. The width of the Gaussian will hence correspond to the coherence time of the atmosphere (or the time taken to sweep through the coherence envelope due to the optical bandwidth, if that is smaller).
The above operation corresponds to convolving the data with the template, which can be easily done in Fourier space. The data is fast Fourier transformed and multiplied by the fast Fourier transform of the template. Fourier transforming back to the time domain gives the correlation of the template with the data.
We can at once convolve with two templates simultaneously, namely the envelope multiplied a cosine function and the envelope multiplied by a sine function, which corresponds to finding the real and imaginary parts of the fringe phasor. Multiplying a one-sided Fourier window function is indeed equivalent to convolving with a real cos function and an imaginary sine function. Taking the modulus squared of the resulting complex correlation therefore gives the total fringe power in these two templates as a function of time. The resulting function is a series of envelopes, which can be folded in time to give an average envelope, and this is what is plotted in Fig. 4.b.
The same process is applied for the three beam case. Instead of using one single template, we use a template for each available baseline. The central frequency of the template is adjusted so as to correspond to the frequency fixed by the sweep amplitude used for a given baseline. As a result, we obtain three envelope functions corresponding to the three simultaneous fringe patterns. This algorithm realises a demodulation of the interleaved fringe signal to restore the OPD information for different fringe frequencies.
Once the fringe envelopes have been computed, we apply a routine based on a centroid calculation to determine the mean position of its centre. This mean position is then used as an estimate of the OPD.
In the one baseline case, we derive one OPD measurement and we have one trolley to move. Whereas in the three baseline case, we got three OPD measurements and two trolleys to move. The extra bit of information is used to better constrain the position of the two trolleys. Each trolley position is derived from the weighted average of the three measured OPDs. This procedure is particularly useful in the case where the fringes on the baseline we are supposed to track on, have a low contrast and can not be detected while the fringes are still detected on the two other baselines (i.e. baseline bootstrapping).

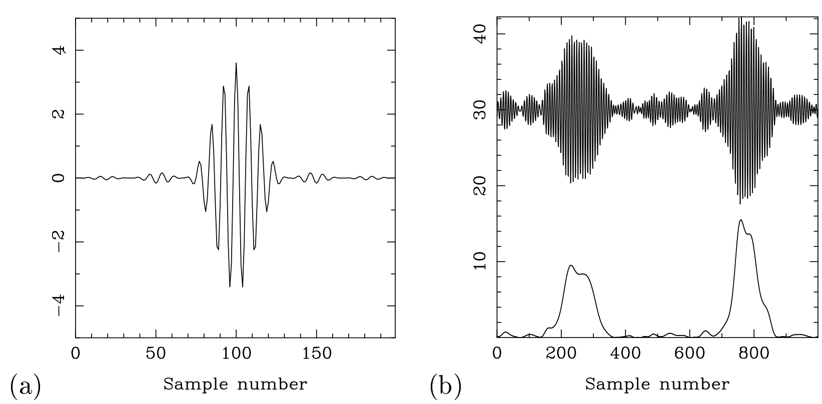

Figure 4. The template function (a). Example of intensity data and the resulting group-delay signal (b).

5. PRELIMINARY RESULTS

The algorithm has been intensively tested using an artificial star to verify the stability of the system and to set the parameters of the closed loop servo. When a suitable set of parameters was defined, the system was ready for tests on the sky. The data analysed here were taken on the 14th of August 2002 with the centre and outer west telescopes, providing a 38m baseline. We observed α Cygni which was chosen because it is a bright (V =1.25)

and not resolved target (angular size = 2.53 mas). The filters used in front of the four APDs were 905nm/50nm, 905nm/50nm, 830nm/40nm and 780nm/30nm. We used the data from an APD with a 780nm filter in front of it for fringe envelope tracking. The mean photon rate was 1.5×10^5photons/s.
We have recorded the data alternatively with and without using the fringe envelope tracker. We have represented in Fig.5 the temporal variation of the envelope position for a few data files. Each plot represents 60s of data, the envelope position being calculated for every second of data. This means that all the variations faster than 1Hz are averaged and do not appear on these plots.
The top panel represents a set of files recorded without the use of the fringe tracker. The fringe envelope motion comprises a low frequency modulation with an amplitude of 40μm and a period of several tens of seconds. As well as a faster modulation with an amplitude of about $5 - 10\mu$m and a period of a few seconds. Another effect observed if we do not track the fringes, but not illustrated here, is a slow drift of the fringe packet due to small errors in the baseline solution. The low frequency of the fringe envelope motion arises from the fact we use a long baseline. As a comparison, Fig. 6 represents the fringe envelope motion recorded while using the centre and east telescopes providing a 10m baseline. The fringe envelope position appears to be pretty stable even without fringe tracking.
The bottom panel in fig. 5 represents a set of files recorded while we were using the envelope tracking system. It appears that the fringe envelope low frequency displacements are very well corrected. The envelope position fluctuates around the null-OPD position. Nevertheless, the high frequency motion is still present with a slightly reduced amplitude. This indicates that the servo is correcting atmospheric motions on timescale of order 5 seconds

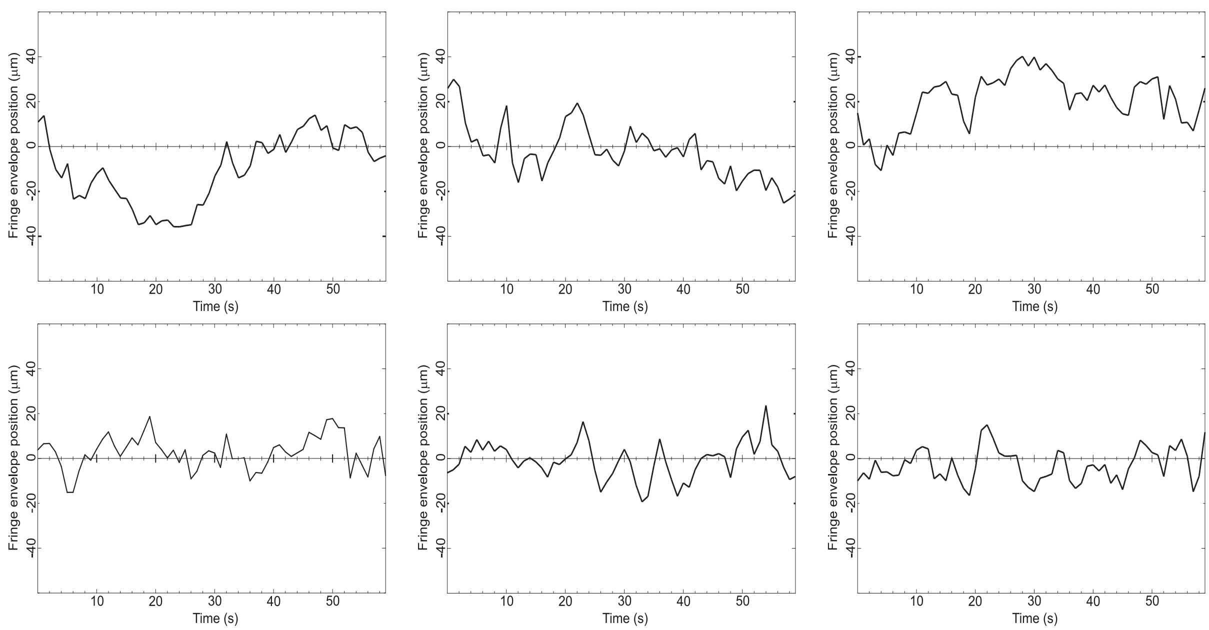

Figure 5. Each plot represents 60s of data. They have been recorded with a 780nm/30nm in front of the APD on the star α Cygni on the 14th of August 2002. The top plots have been recorded while not using the fringe tracking system. The vertical axis has a 60μm amplitude.

6. MULTI-CHANNEL ENVELOPE TRACKING

At the moment, the fringe envelope tracking system uses the signal from one single APD. However, we may want to use all the available information to determine the trolley offsets. The main difficulty arises from the use of different spectral filters for the different APDs.

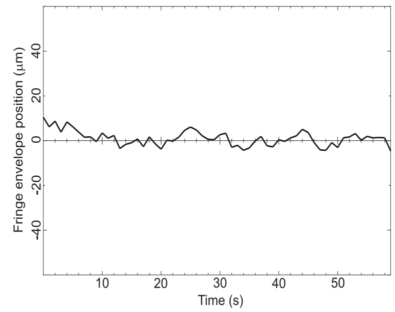

Figure 6. Motion of the fringe envelope recorded on the 28th of August on α Lyrae. We used the centre and east telescopes providing a 10m baseline and a 780nm/30nm filter in front of the APD. The average photon rate for this file was about 1.75×10^5 photons/s. The plot represents 60s of data . The vertical axis has a 60μm amplitude.

Fig. 7 represents the temporal variation of the fringe envelope motion recorded on the four APDs. Each data point is the envelope position averaged over one second of data. The upper most curve is the plot of the envelope position calculated with data from APD4 which was used for fringe tracking. We can see that the envelope position recorded for this APD fluctuate around the null-OPD position whereas the envelope positions estimated with data from the other APDs are shifted from the null-OPD. The shift is larger as the wavelength difference between the spectral filters is bigger.
These shifts are due to the longitudinal dispersion effect which arises because we compensate the optical path delay in the air and not in vacuum. The data represented in figure 7 lead to three different optical path difference estimates of 0μm , -10μm and -20μm.
If we want to use this information for fringe tracking, we will either need to develop a model of the longitudinal dispersion for COAST or use spectral filters which have bandpaths close enough for the dispersion effect to be negligible. In both cases the use of the signal from the four APDs would provide a better estimate of the optical path fluctuations.

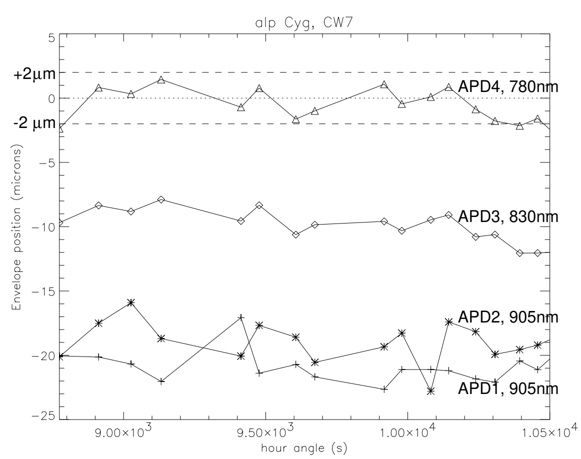

Figure 7. Fringe envelope motion versus time. Each point represents the envelope position averaged over 60s of data. The four curves represent the date coming out from the four different APDs. From top to bottom: APD4 with a 780nm/30nm filter, APD3 with an 830nm/40nm filter, APD2 with a 905nm/50nm filter and APD1 with the same filter as APD2.

7. TEST AT IOTA

We have established a collaboration with the Infrared-Optical Telescope Array (IOTA) group for the development of fringe tracking algorithms. The idea was to develop algorithms which can be tested and used both at COAST and IOTA in order to carry out a study on their respective efficiency and limitations and establish which algorithm is the most suitable for low light level observations.

E. Pedretti developed and installed the IOTA fringe tracking system. The algorithm he developed is based on the measurement of the complex phase of the Fourier transform of the fringe pattern and is routinely used at IOTA. This system will be described in a forthcoming publication.

Tests were carried out at IOTA to compare the two algorithms. They have been used to tack fringes on the star α Vul, in the H band, with a 5.5m baseline. We represent in figure 8 the data recorded with the COAST algorithm. The COAST algorithm behaved very well even if the IOTA algorithm proved to be less time consuming in its execution.

No conclusion has yet been made regarding their respective efficiency since the two algorithms have so far showed similar results for fringe tracking. Further investigation is required to quantify their efficiency.

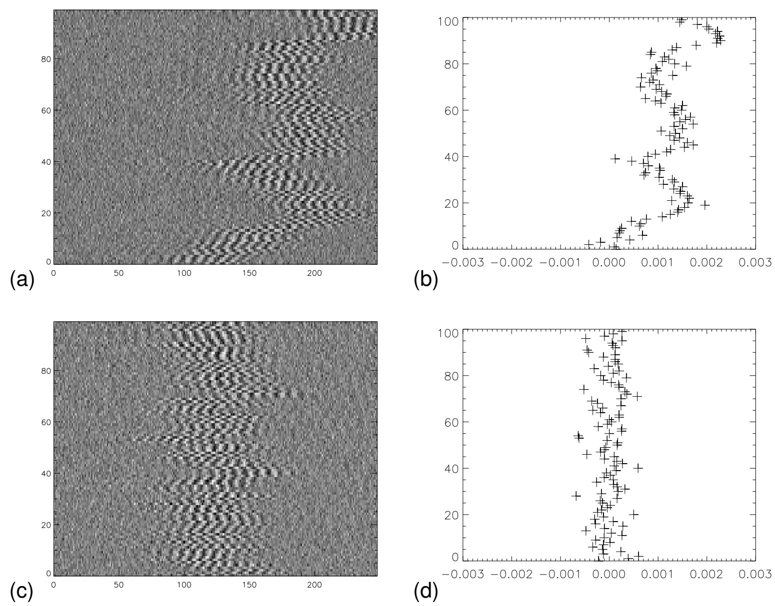

Figure 8. Fringes from the IOTA IONIC3T combiner on the PICNIC camera recorded in the H band on the star α Vul with a 5.5m baseline. (a) Fringe pattern recorded without fringe tracking. (b) Fluctuations of the position of the fringe packet represented in (a). (c) Fringe pattern recorded while using the fringe envelope tracking developed at COAST. (d) Corresponding fringe packet position.

8. CONCLUSION

We have been able to implement a fringe envelope tracking system at COAST. This system has been successfully tried on the sky. It managed to keep the fringe packet around the null-OPD position.The next step will be to enable the system to work with 4 incoming beams. In this case, we will have to compute 6 fringe envelopes to derive 6 different OPDs and control three trolleys. We will also try the fringe tracker with data from the infrared beam combiner. A detailed study of the performances and limitation of the different algorithms will be carried out. The purpose of this study is be to determine the relative merits of the two algorithms and characterise their performance at low light levels. According to the results we may decide to choose one or the other algorithm or even switch from one to the other according to the observing circumstances.

ACKNOWLEDGMENTS

This research was made possible thanks to a Marie Curie Fellowship (within the Fifth Framework programme "Improving Human Research Potential and the Socio-economic Knowledge Base) granted to N. D. Thureau (contract HPMF-CT-200-00966).

REFERENCES

1. C. A. Haniff, J. E. Baldwin, A. G. Basden, N. A. Bharmal, R. C. Boysen, D. F. Busher, A. V. George, J. W. Keen, C. D. Mackay, B. O'Donovan, D. Pearson, J. Rogers, E. B. Senata, H. Thorsteinsson, N. Thureau, R. N. Tubbs, P. J. Warner, D. M. Wilson, and J. S. Young, "Pogress at COAST 2000-2002," in *Interferometry for optical astronomy II*, W. A. Traub, ed., *Proc. SPIE* **4838**, 22–23 Aug. 2002 Waikoloa, Hawaii USA, SPIE, 2002.
2. A. V. George, J. E. Baldwin, R. C. Boysen, C. A. Haniff, C. D. Mackay, D. Pearson, J. Rogers, P. J. Warner, D. M. Wilson, and J. S. Young, "Performance of new fringe-detecting avalanche photodiodes at COAST," in *Interferometry for optical astronomy I*, P. J. Lena and A. Quirrenbach, eds., *Proc. SPIE* **4006**, p. 556, 27–29 Mar. 2000, Munich, SPIE, 2000.
3. J. S. Young, J. E. Baldwin, M. G. Beckett, R. C. Boysen, C. A. Haniff, P. R. Lawson, C. D. Mackay, J. Rogers, D. St-Jacques, P. J. Warner, and D. M. A. Wilson, "COAST in the near-infrared: solutions for infrared interferometry," in *Astronomical Interferometry*, R. D. Reasenberg, ed., *Proc. SPIE* **3350**, p. 746, 20–24 Mar. 1998, Kona, Hawaii, SPIE, 1998.